

7th Scientific-Technical Conference Material Problems in Civil Engineering (MATBUD'2015)

The examination of the Glass Fiber Reinforced Polymer composite rods in terms of the application for concrete reinforcement

Bogusław Jarek^{a,*}, Aleksandra Kubik^a

^a*Cracow University of Technology, Warszawska 24, 31-155 Kraków, Poland*

Abstract

GFRP (Glass Fiber Reinforced Polymer) rods have found a wide range of applications in building structures as reinforcement of concrete bearing elements. In no time on the market appeared a few producers who are offering a wide assortment of diameters. In this paper, applied test procedures and their results for GFRP rods are presented. Rods made by three manufacturers, with declared diameter 12 mm, have been analyzed. The tensile strength, elasticity modulus and ultimate limit strain, based on the static tensile test, were compared. These resultants were compared with tensile strength obtained for widespread use reinforcement steel AIIIIN. Different results of composite rods destroying process are discussed. It worth stressing the great discrepancy between the declared and real diameter of tested rods, which may result in an inability to simple conversion between conventional steel reinforcement to composites in structural elements.

© 2015 Published by Elsevier Ltd. This is an open access article under the CC BY-NC-ND license (<http://creativecommons.org/licenses/by-nc-nd/4.0/>).

Peer-review under responsibility of organizing committee of the 7th Scientific-Technical Conference Material Problems in Civil Engineering

Keywords: GFRP rods; composite; composite reinforcement; static tensile test; glass fiber

1. Introduction

Composite rods made of glass fibers are widely used especially in the engineering construction [1] in harsh environmental conditions, where high corrosion resistance as well as good thermal, electrical and electromagnetic insulation are required. They are widely used in geotechnical engineering as reinforcing land components (in the

* Corresponding author. Tel.: +48-12-628-29-10; fax: +48-12-628-20-24.
E-mail address: bjarek@pk.edu.pl.

form of reinforcement mesh) or slope protection elements, embankments, rock mass - as ground anchors. Because of low density of the composite (in relation to steel), which results in ease of transport and less time required to reinforce concrete structure components, they are used as reinforcement in general, road and tunnel construction [2,3]. The growing area and low cost of application of composite rods has resulted in a wide range of products which can be an alternative to steel reinforcement [4]. Reducing the amount of reinforcement in case of changing steel reinforcement into composite one is possible, but it requires experience and expertise. On the market there are several manufacturers offering reinforcement rods made of glass fibers (GFRP), so it was decided to compare their basic mechanical properties based on a sample of axial rods stretching with a diameter of 12 mm.

2. Methodology of examination

A static tensile test was used to determine the mechanical properties of the GFRP rods. Due to the absence of standards and guidelines for testing fiber reinforced composite rods in Poland, the provisions of PN-EN ISO 6892-1:2010 standard concerning methods for testing metals in terms of stretching were used during the research. This approach allowed a direct comparison of the properties of GFRP rods with ordinary steel reinforcement rods.

Static tensile test of the GFRP rods was carried out in the Research Laboratory for Materials and Construction Structures at Cracow University of Technology, using the Zwick/Roell Z1200 machine. The samples properly prepared and mounted in the jaws of the tensile machine were subjected to an axial tensile force. The test was carried out until braking rod. The load was increased at the constant rate of 10 MPa/s. The tests were performed at ambient temperature i.e. about 20°C.

The rods provided for testing with a nominal diameter of 12 mm have a non-uniform surface over the entire length of the bar both in the core and including the braid. The diameter of the rods was measured in the core without a braid. Due to the presence of the braid and a large scatter of measurements results to calculate the strength characteristics, a circular section of the rods of d_m equivalent diameter was adopted. It was calculated on the basis of the arithmetic average of six measurements made in two perpendicular directions – three measurements in each. The equivalent diameter was the basis for the calculation of stresses and for determining the oblong elasticity module. The results of bar diameters measurements are presented in Table 1.

Table 1. The measurement results of the rods diameter.

	Component designation	diameter [mm]						Equivalent diameter d_m [mm]	Cross-sectional area A_f [cm ²]
		d_{11}	d_{12}	d_{13}	d_{21}	d_{22}	d_{23}		
Manufacturer 1	Pr 1	10.86	10.82	10.84	10.66	10.69	10.74	10.8	0.91
	Pr 2	10.88	10.89	10.88	10.83	10.80	10.81	10.8	0.92
	Pr 3	10.98	11.00	10.99	10.78	10.80	10.79	10.9	0.93
	Pr 4	10.77	10.76	10.73	10.60	10.73	10.70	10.7	0.90
	Pr 5	10.97	10.02	11.00	10.61	10.73	10.72	10.7	0.89
Manufacturer 2	Pr 1	12.80	12.80	12.82	12.80	12.78	12.75	12.8	1.28
	Pr 2	12.70	12.78	12.73	12.69	12.67	12.70	12.7	1.27
	Pr 3	12.82	12.80	12.83	12.81	12.80	12.80	12.8	1.29
	Pr 4	12.75	12.76	12.75	12.80	12.81	12.76	12.8	1.28
	Pr 5	12.74	12.79	12.80	12.80	12.76	12.78	12.8	1.28
Manufacturer 3	Pr 1	13.75	13.70	13.75	13.76	13.75	13.70	13.7	1.48
	Pr 2	13.50	13.67	13.50	13.81	13.80	13.76	13.7	1.47
	Pr 3	13.60	13.57	13.95	13.60	13.64	13.60	13.7	1.46

Figure 1 shows the test stand with a composite bar fitted in the tensile machine, before starting axial stretching.

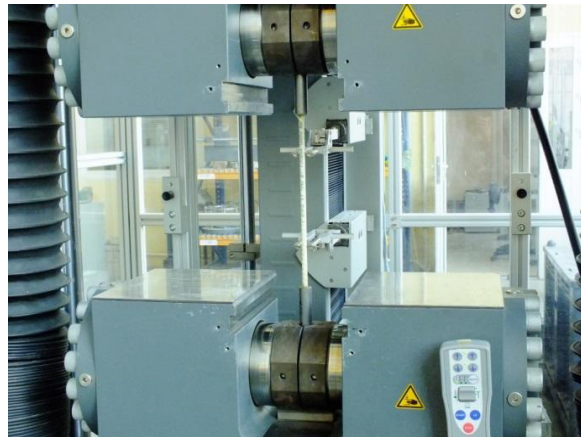


Fig. 1. Test stand for static tensile test.

As it follows from the presented measurements, the difference between the nominal diameter (12 mm) and the equivalent diameter ranges from -11% to + 14%, which makes a difference between the diameters of the rods of each manufacturer of nearly 3 mm, i.e. 25% of the nominal diameter.

The axial tensile strength of the rod f_f assumed the stress corresponding to the maximum tensile force F_m , obtained during the tensile test. This value is related to the initial circular cross-section. In addition, the deformation was determined as $\varepsilon = \Delta l / l_0$ where l_0 is the length of the measurement section before the test and Δl is the elongation of the sample at the measuring section. Elongation Δl was determined using an extensometer, which is provided in the testing machine.

Young's Modulus of elasticity E_f in tension was determined by the software servicing the testing machine - testXpert II. Young's Modulus is defined as the angle tangent between the secant diagram and elongation axis at the moment the sample obtains the stress between 100 MPa and 500 MPa.

The value of deformation ε_f , which corresponds to maximum stress, was adopted as boundary deformation.

3. Research findings

During the static tensile test the load and deformation of the sample were recorded. The results are shown in the graphs $\sigma - \Delta l$ (stress – relative elongation). On the basis of the results obtained, according to the formulas given in the previous section, the breaking strength value, Young's modulus and boundary deformation were calculated. Additionally, the manner of degradation of the sample was noted.

3.1. Manufacturer 1

The rods consist of glass fibers arranged in parallel, embedded in vinyl - ester resin, of circular section, and the entire outer surface is shaped as a trapezoidal thread (Fig. 2b) with a profile depth of not less than 0.75 mm and a thread pitch of 8 mm. As a result of the manufacturing process the finished rods have grooved ribs, which results in discontinuity of fibers on the outer surface.

The results of individual tensile tests are shown in Fig. 2a. The tested rods demonstrate a non-linear relationship between stress and deformation in the entire load range. This non-linearity can be a result of resin matrix cracking.

After reaching the maximum stress, one can note braking next fibers and the remaining fibers taking over the load, followed by the destruction of the entire cross-section of the bar.

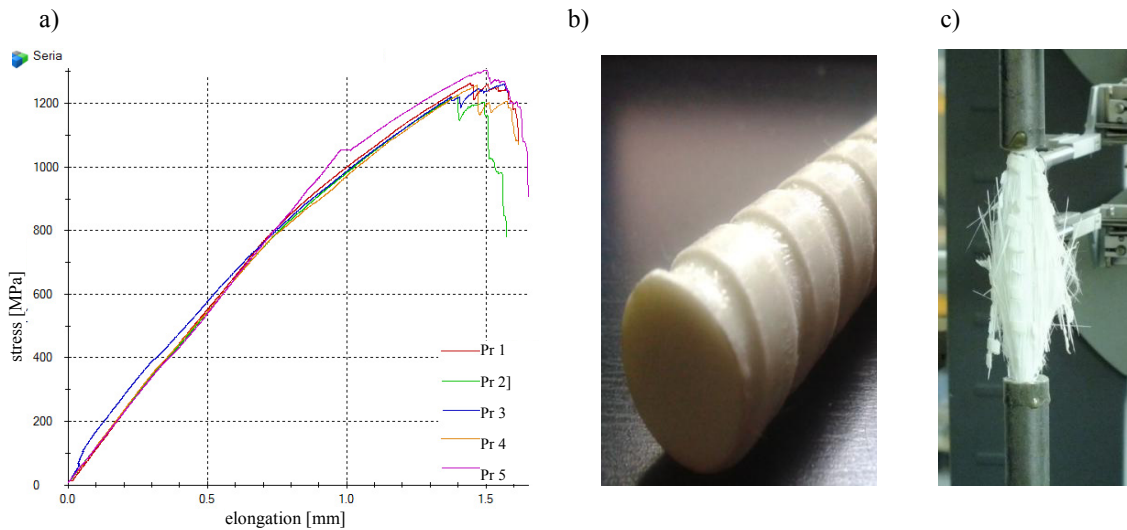


Fig. 2. Manufacturer 1: (a)Chart $\sigma - \Delta l$ for GRFP rods; (b) Composite fiber glass bar; (c) The form of bar destruction.

Based on the examination carried out, it can be concluded that the average axial tensile strength of the rods is 1268.5 MPa. The average modulus of elasticity E_f is equal to 54.0 GPa and the average boundary deformation is 2.4%.

The destruction of the rods was caused by progressive fracture toughness of subsequent fibers, accompanied by a partial loss of strength. First matrix cracking was occurred. Then was broken fibers. The destruction occurred suddenly. Just before the destruction, breaking matrix cracks could be heard. After the destruction, unfettered glass fibers take the form of "spatial plume" (Fig. 2c).

Table 2 shows the results of strength tests of rods made by manufacturer 1.

Table 2. Results for rods strength tests - manufacturer 1.

labelling	Destructive force F_m	Breaking stress f_f	Average tensile strength f_{fm}	Modulus of elasticity E_f	Average modulus of elasticity E_{fm}	Boundary deformation ϵ_f	Average boundary deformation ϵ_{fm}
-	[kN]	[MPa]	[MPa]	[GPa]	[GPa]	[%]	[%]
Pr 1	162.24	1267.5		56		2.26	
Pr 2	157.80	1242.5		53		2.34	
Pr 3	162.21	1257.4	1268.5 ± 26.0	54	54.0 ± 1.2	2.33	2.4 ± 0.08
Pr 4	161.71	1263.4		54		2.34	
Pr 5	167.91	1311.8		53		2.48	

3.2. Manufacturer 2

The glass fiber rods are made using pultrusion method in epoxy resin, they are of circular section with additional braiding of one-sided turning profile (Fig. 3b). The resin, which is the matrix for the glass fibers on the rods side surface, demonstrates highly variable geometry.

The graphs of individual tensile tests are shown in Fig. 3a and the tensile test results are presented in Table 3. The tested rods demonstrate a linear relationship between stress and deformation to obtain stresses of approx. 300 MPa (corresponding to approx. 25% of the characteristic tensile strength). In the next stretching step, this relationship is non-linear until the maximum stress is obtained. After breaking the first fibers, the load is taken over by the working part of the bar section, which is accompanied by a slight decrease in capacity.

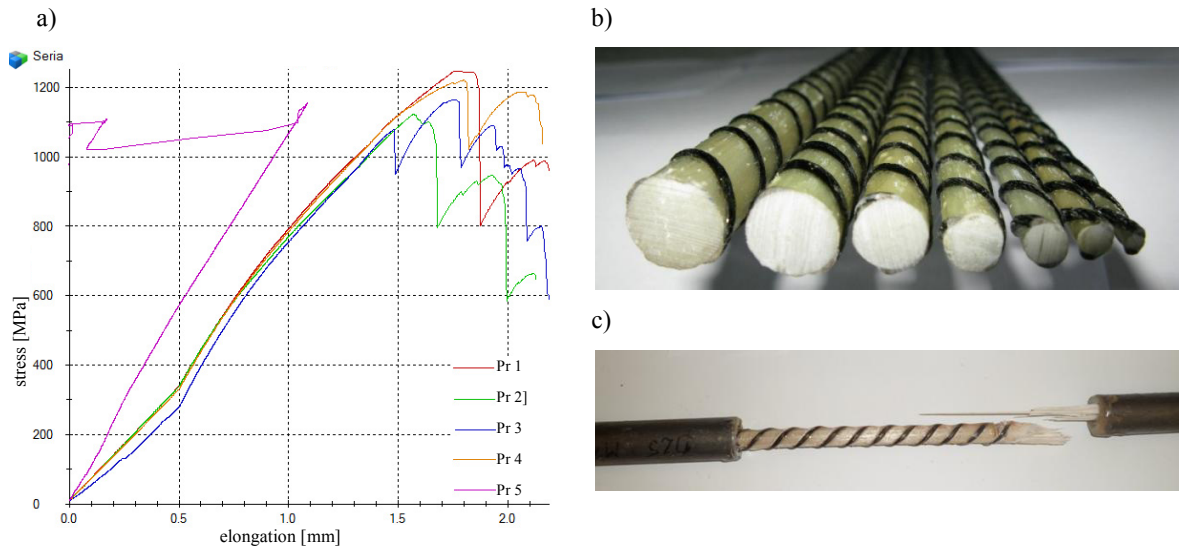


Fig. 3. Manufacturer 2: (a) Chart $\sigma - \Delta l$ for GRFP rods; (b) Composite fiber glass bar; (c) The form of bar destruction.

Table 3. Results for rods strength tests - manufacturer 2.

labelling	Destructive force F_m	Breaking stress f_f	Average tensile strength f_{fm}	Modulus of elasticity E_f	Average modulus of elasticity E_{fm}	Boundary deformation ε_f	Average boundary deformation ε_{fm}
-	[kN]	[MPa]	[MPa]	[GPa]	[GPa]	[%]	[%]
Pr 1	114.18	1254.7		56		2.24	
Pr 2	102.79	1117.3		53		2.11	
Pr 3	106.58	1146.0	1190.0 ± 68.5	54	54.3 ± 1.3	2.12	2.2 ± 0.09
Pr 4	111.76	1241.8		54		2.30	
Pr 5	105.74	1188.1		53		2.24	

The results for element Pr 5 have been omitted in the calculations due to unusual behavior of the tested component. The rods made by manufacturer 2 reached an average axial tensile strength of 1190.0 MPa, cutting E_{fm} elasticity modulus is 54.3 GPa and the average boundary deformation is equal to 2.2%.

The destruction of the rods was caused by breaking the adhesion between the braiding and the bar core. Subsequently, breaking the next fibers proceeded. The destruction form is compact (Fig. 3c).

3.3. Manufacturer 3

The rods made using the pultrusion method are composed of continuous glass fibers embedded in a thermosetting synthetic resin. In addition, the rods are reinforced with braiding, and their entire external surface is covered with a grippy sand. The rod surface is rough. The rod has "rotund" - variable cross sections - wherein it is the narrowest at the braiding and the widest in the middle of the section between the braids (Fig. 4b).

The tested rods demonstrate a linear relationship between stress and deformation to obtain stresses of approx. 500 MPa (corresponding to approx. 67% of the characteristic tensile strength). In the next stretching step, this relationship is non-linear until the maximum stress is obtained. The graph does not demonstrate any transfer of the load onto the next fibers. After crossing the maximum stress, a rapid decline in the rod capacity takes place. The chart $\sigma - \Delta l$ for the research components of manufacturer 3 is presented in Fig. 4a. Table 4 summarizes the values of the obtained material properties.

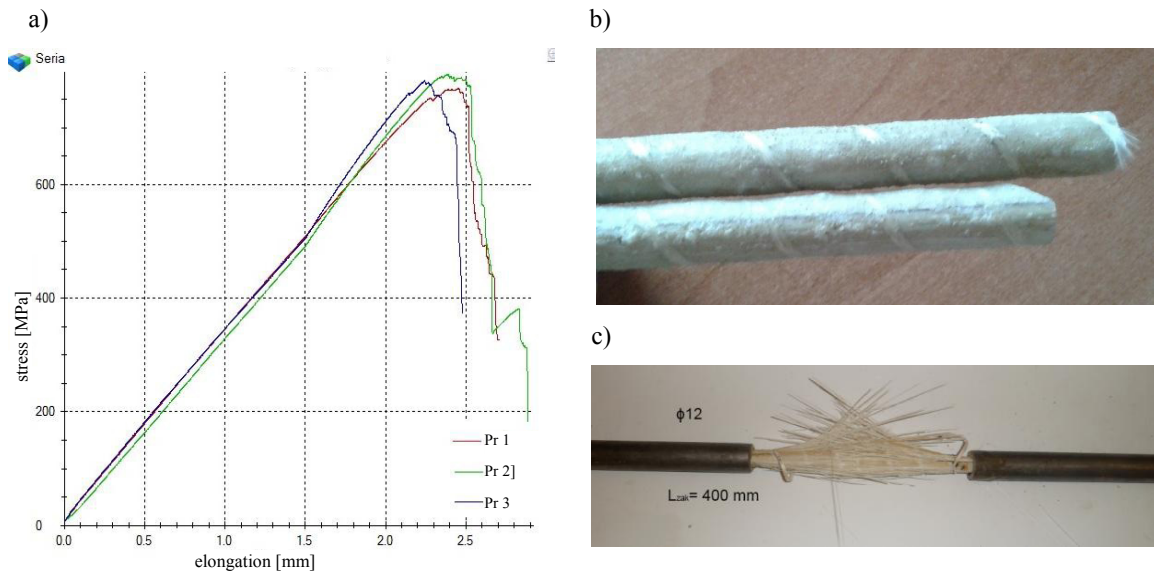


Fig. 4. Manufacturer 3: (a) Chart $\sigma - \Delta l$ for GRFP rods; (b) Composite fiber glass bar; (c) The form of bar destruction.

Table 4. Results for rods strength tests - manufacturer 3.

labelling	Destructive force F_m	Breaking stress f_f	Average tensile strength f_{fm}	Modulus of elasticity E_f	Average modulus of elasticity E_{fm}	Boundary deformation ε_f	Average boundary deformation ε_{fm}
-	[kN]	[MPa]	[MPa]	[GPa]	[GPa]	[%]	[%]
Pr 1	113.25	764.7		40		1.91	
Pr 2	116.90	796.5	782.8 ± 16.3	39	39.3 ± 0.6	2.04	2.0 ± 0.08
Pr 3	115.31	787.2		39		2.02	

The axial tensile strength of rods $\phi 12$ of Manufacturer 3 is 782.8 MPa. The average secant modulus of elasticity is 39.3 GPa and the average boundary deformation is equal to 2.0%.

The destruction of the rods took place in the same way as in the case of the rods of manufacturer 1, i.e. by cracking of the subsequent fibers. The detachment of the braiding from the bar core was noticeable. The destruction was accompanied by a decrease of strength, and its nature is shown in Fig. 4c.

4. Summary

1. The dependence of $\sigma - \Delta l$ for rods of each manufacturer was non-linear. For two types of rods (made using the pultrusion method), in the diagrams straight sections of different lengths are distinguished. This means that with increasing load, beyond certain load limits (different for each rod) Young's modulus changes. The boundary

point occurs where the glass fiber matrix is destroyed and the entire strength is transferred by glass fibers only. Further part of the graph is non-linear due to the destruction of individual fibers. In the case of rods of manufacturer 1 the graph $\sigma - \Delta l$ is non-linear in its entire range. It is worth noting that the results for rods of each manufacturer are highly consistent.

2. The essential difference between different types of GFRP rods was the nature of their destruction. The rods of manufacturer 1 and 3 were destroyed similarly – by brittle fracture of the subsequent fibers in the middle of measurement section which, together with the load increase, resulted in crumbling the resin matrix and an increase in the volume of fibers, creating the form resembling a "plume". The different nature of the destruction was demonstrated by the rods of manufacturer 2. Initially, the rod braiding destroyed itself, which was followed by resin cracking along the fiber. The final form of degradation was to break the continuity of the fibers within the core, which caused the separation of the rod into two parts, without increasing the volume in the measuring section. Such methods of destruction are reflected in the graphs $\sigma - \Delta l$. In the case of manufacturers 1 and 3, there is very small relative elongation after reaching the maximum stress – characteristic of the brittle fracture of the composite. The rods of manufacturer 2 indicated the beginning of the destruction by breaking the braiding (the first peak on the graph), and only at a later stage exhaustion of glass fiber carrying capacity followed (the second peak and subsequent ones).

3. In Fig. 5 below, a comparison of the results of the axial tensile strength for the three tested types of AIIIN steel and GRFP rods is presented.

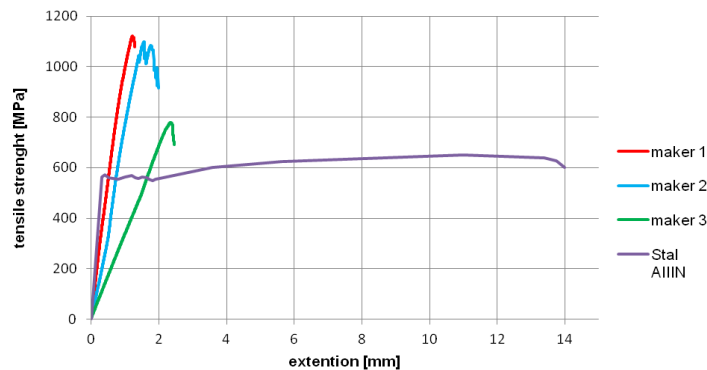


Fig. 5. Chart $\sigma - \Delta l$ for GRFP and steel rods.

For the two types of rods, the bearing capacity of the GFRP rods was more than twice as high as for AIIIN steel. For the third type of rods, their load capacity was higher by about 30%. Young's modulus for manufacturers 1 and 2 was 54GPa, and in the case of a manufacturer 3 - 39GPa.

4. The diameters of the rods tested showed significant scatter of results over the entire length of the rods in two perpendicular directions. All rods had a shape similar to a circular cross-section rather than circular. The declared diameter (nominal) by the manufacturer differed by as much as about 20% from the actual one (equivalent). The tests have confirmed that it is not true to say that the bar bearing capacity increases with increasing diameter. Bar carrying capacity depends on the type of glass fibers, the matrix (resin), but also the method of production.

5. The use of rods made of glass fibers, owing to their much greater bearing capacity than the steel ones, seems to be a matter of time. The attempts made encourage such actions, but one cannot uncritically replace steel rods with those made of glass fiber being guided only by their diameter. Careful attention should be paid to the

information contained in the manufacturer's product cards because, as proved by the tests, with the same nominal diameter the capacity results and Young's modulus can vary significantly.

References

- [1] Szumigala M., Pawłowski D, Application of composite rodsrebar in building structures. *Przegląd Budowlany* 3/2014, p. 47-50 (In Polish)
- [2] Stankiewicz B., The replacement of the traditional steel reinforcement by composites with glass fiber. *Szko i Ceramika. ROCZNIK* 60 (2009), p.33-37.
- [3] Benmokrane B., Chaallal O., Masmoudi R. Glass Fibre Reinforced Plastic (GFRP) Rebars for Concrete Structures. *Construction and Building Materials*, Vol.9, No.6 pp. 353-364, 1995
- [4] Berg A.C., Bank L.C., Oliva M.G., Russell J.S., Construction and Cost Analysis of an FRP Reinforced Concrete Bridge Deck. *Construction and Building Materials*. 7 April 2005.